Dephosphorylation by Default, a Potential Mechanism for Regulation of Insulin Receptor Substrate-1/2, Akt, and ERK1/2[*]

Rachel Zhande[‡1], Wenshuo Zhang[‡], Yanbin Zheng[‡], Elisha Pendleton[‡], Yu Li[§], Roberto D. Polakiewicz[§], and Xiao Jian Sun[‡2]

From the [‡]Section of Endocrinology, The University of Chicago, Chicago, Illinois 60637 and [§]Cell Signaling Technology, Incorporated, Beverly, Massachusetts 01915

Protein phosphorylation is an important mechanism that controls many cellular activities. Phosphorylation of a given protein is precisely controlled by two opposing biochemical reactions catalyzed by protein kinases and protein phosphatases. How these two opposing processes are coordinated to achieve regulation of protein phosphorylation is unresolved. We have developed a novel experimental approach to directly study protein dephosphorylation in cells. We determined the kinetics of dephosphorylation of insulin receptor substrate-1/2, Akt, and ERK1/2, phosphoproteins involved in insulin receptor signaling. We found that insulin-induced ERK1/2 and Akt kinase activities were completely abolished 10 min after inhibition of the corresponding upstream kinases with PD98059 and LY294002, respectively. In parallel experiments, insulin-induced phosphorylation of Akt, ERK1/2, and insulin receptor substrate-1/2 was decreased and followed similar kinetics. Our findings suggest that these proteins are dephosphorylated by a default mechanism, presumably via constitutively active phosphatases. However, dephosphorylation of these proteins is overcome by activation of protein kinases following stimulation of the insulin receptor. We propose that, during acute insulin stimulation, the kinetics of protein phosphorylation is determined by the interplay between upstream kinase activity and dephosphorylation by default.

The reversible phosphorylation of proteins has emerged as a major mechanism for the regulation of cellular signal transduction (1, 2). Disruption of protein phosphorylation/dephosphorylation has been linked to many pathological conditions, including cancer, neurodegeneration, diabetes, cystic fibrosis, asthma, and cardiovascular disease (3–5). Despite the critical importance of protein phosphorylation in signaling and disease, the underlying mechanisms that determine the kinetics of

dephosphorylation remain unresolved. Two general models have been proposed to describe these mechanisms. One model posits that the phosphorylation level is determined by constitutively active phosphatases and transiently activated kinases (2, 6). This model was established based on results gathered using potent phosphatase inhibitors such as okadaic acid on intracellular proteins as well as in *in vitro* cell-free assays. Therefore, although it is an attractive explanation, it may not reflect mechanisms operative in intact living cells. A second model based on studies employing advanced molecular techniques conducted in both animals and genetically engineered cell lines suggests that both kinases and phosphatases are coordinately regulated (3, 7–10). However, most of these studies assessed protein dephosphorylation in the presence of upstream kinase activity; therefore, potential influences from constitutively active phosphatases may have been hidden and thus overlooked.

Methods to directly measure protein dephosphorylation *in vivo* in the absence of upstream kinase activity are lacking. As a result, despite the aforementioned studies, we still do not know the relative contribution of inducible and constitutively active phosphatases in determining the phosphorylation state of key protein effectors in receptor-mediated signaling cascades.

Insulin signaling is controlled by phosphorylation/dephosphorylation of many phosphoprotein effectors downstream of the insulin receptor (11). After binding insulin, the intrinsic tyrosine kinase in the β-subunit of the insulin receptor activates and phosphorylates diverse substrates, including insulin receptor substrate (IRS)[3]-1 and IRS-2. Phosphoinositol 3-kinase (PI3K) is activated following recruitment to phosphorylated IRS-1/2 and leads to the phosphorylation and activation of Akt (also known as protein kinase B) (12–14). Phosphorylated IRS-1/2 also induces activation of MEK, leading subsequently to phosphorylation of ERK1 and ERK2, members of the MAPK family (15–17).

Although the insulin-induced phosphorylation of IRS-1/2, Akt, and ERK1/2 is well characterized, the mechanisms that

---

[1] Present address: Dept. of Medical Biophysics, British Columbia Cancer Research Center, Vancouver, British Columbia V5Z 1L3, Canada.
[2] To whom correspondence should be addressed: The University of Chicago, M-266, MC1027, 5841 S. Maryland Ave., Chicago, IL 60637. Tel.: 773-702-9661; Fax: 773-834-0486; E-mail: xsun@medicine.bsd.uchicago.edu.

[3] The abbreviations used are: IRS, insulin receptor substrate; PI3K, phosphoinositol 3-kinase; MEK, mitogen-activated protein kinase/extracellular signal-regulated kinase kinase; ERK, extracellular signal-regulated kinase; MAPK, mitogen-activated protein kinase; CHO, Chinese hamster ovary; IR, insulin receptor; HA, hemagglutinin; HNMPA-(AM)₃, hydroxyl-2-naphthalenylmethylphosphonic acid trisacetoxymethyl ester; DTT, dithiothreitol; TBS, Tris-buffered saline; SGK, serum- and glucocorticoid-inducible kinase; PP, protein phosphatase.

control the dephosphorylation of these signaling molecules are not definitively known. To determine whether activation of phosphatases is required for protein dephosphorylation, we developed a novel experimental approach to directly determine the dephosphorylation rate in living cells. Cells were stimulated with insulin to induce maximum protein phosphorylation. Then, well defined protein kinase inhibitors were added, and the rates of dephosphorylation of IRS-1/2, Akt, and ERK1/2 were determined. Our findings reveal the existence of a potential mechanism whereby downstream effectors of insulin signaling are dephosphorylated, unless upstream kinases are active. We refer to this observation as "dephosphorylation by default."

EXPERIMENTAL PROCEDURES

Cell Culture—Chinese hamster ovary (CHO) cells overexpressing the wild-type human insulin receptor (IR), rat IRS-1, and hemagglutinin (HA)-tagged mouse Akt (CHO/IR/IRS-1/HA-Akt cells) were grown in nutrient mixture F-12 supplemented with 10% fetal bovine serum (18). H2.35 cells (American Type Culture Collection) were grown in low glucose Dulbecco's modified Eagle's medium supplemented with 4% fetal bovine serum and 200 nM dexamethasone (19, 20). Primary hepatocytes were grown in growth medium (50% high glucose Dulbecco's modified Eagle's medium, 40% nutrient mixture F-12, 10% fetal bovine serum, 10 nM dexamethasone, and 100 units/ml penicillin/streptomycin). All cells were maintained at 37 °C in a humidified atmosphere with 95% air and 5% CO_2. At 80% confluence, cells were fasted in serum-deprived high glucose Dulbecco's modified Eagle's medium supplemented with 0.25% bovine serum albumin for 16 h (CHO and H2.35 cells) or 6 h (primary hepatocytes) and then incubated with or without insulin (100 nM) for the indicated times (21). Inhibitors, including sodium orthovanadate (500 μM), hydroxyl-2-naphthalenylmethylphosphonic acid trisacetoxymethyl ester (HNMPA-(AM)$_3$; 500 μM), LY294002 (50 μM), and PD98059 (250 μM), were added at the indicated times before or after addition of insulin. At the end of treatment, cells were lysed in Laemmli sample buffer containing 0.1 M dithiothreitol (DTT) for immunoblot analysis or in lysate buffer (see below) for immunoprecipitation.

Primary Hepatocyte Isolation—Mouse primary hepatocytes were isolated using a modified protocol according to Klaunig *et al.* (22, 23). The liver was perfused with calcium and magnesium-free Hanks' buffered salt solution (Invitrogen) supplemented with EGTA (prewarmed to 37 °C and gassed with 95% O_2 and 5% CO_2) for 4 min at a rate of 4 ml/min, followed by Hanks' buffered salt solution supplemented with 5.9 mM CaCl$_2$ and 0.025 mg/ml Blendzyme III (Roche Diagnostics) for 5 min at a rate of 4 ml/min. The digested liver was excised rapidly, and hepatocytes were released with gentle shaking of the digested liver into 15 ml of chilled (4 °C) hepatocyte isolation medium (high glucose 50% Dulbecco's modified Eagle's medium, 40% nutrient mixture F-12, 10% fetal bovine serum, 100 nM dexamethasone, and 100 units/ml penicillin/streptomycin). Cells were then filtered through a 70-μm nylon filter (BD Biosciences) into a 50-ml conical tube and washed twice with the same medium by centrifugation at 50 × g for 2 min at 4 °C. After

washing, the cells were resuspended in 10 ml of hepatocyte isolation medium. Cell viability was assessed via trypan blue staining and was >85%. cells (3.5 × 10^5/well) were plated in a collagen-coated 12-well plate. After allowing the cells to attach for 2 h at 37 °C, they were washed once, and the medium was replaced with growth medium.

Immunoblot Analysis—For whole cell lysate immunoblotting, cells were lysed directly in Laemmli sample buffer containing 0.1 M DTT and sonicated. Proteins in whole cell lysates were further denatured by boiling for 5 min, separated by SDS-PAGE using 7.5 or 10% gels, and transferred to nitrocellulose membranes. Membranes were blocked overnight at 4 °C in Tris-buffered saline (TBS; 20 mM Tris-HCl (pH 8.0) and 0.15 M NaCl) with 0.05% Tween 20 (TBST) containing 5% milk and then incubated for 1 h at room temperature with anti-IRS-1 or anti-IRS-2 antibody (catalog nos. 420292 and 420293, EMD Biosciences), anti-HA antibody (clone F-7, Santa Cruz Biotechnology, Inc.), anti-Akt phospho-Ser^{473} antibody (catalog no. 9271, Cell Signaling Technology, Inc.), anti-phospho-p44/42 MAPK antibody (catalog no. 9101, Cell Signaling Technology, Inc.), or anti-ERK2 antibody (clone C-14, Santa Cruz Biotechnology, Inc.) according to the manufacturers' recommendations. Following incubation with antibodies, membranes were washed three times with TBST and then probed with horseradish peroxidase-conjugated protein A (Santa Cruz Biotechnology, Inc.) at a 1:3000 (v/v) dilution for 30 min. For the detection of tyrosine phosphorylation, membranes were directly probed with horseradish peroxidase-conjugated antibodies PY20 and PY99 (Santa Cruz Biotechnology, Inc.) at a 1:3000 (v/v) dilution for 30 min. Membranes were washed with TBST and TBS and developed with SuperSignal^{TM} substrate (Pierce) for 5 min. Bands were detected by exposing the membranes on Kodak BioMax MR film (18).

Immunoprecipitation—Cells were washed with buffer A (20 mM Tris-HCl (pH 7.5), 137 mM NaCl, 1 mM CaCl$_2$, 1 mM MgCl$_2$, and 100 μM Na$_3$VO$_4$) and lysed in 1 ml of lysate buffer A (buffer A containing 1 mM phenylmethylsulfonyl fluoride, 100 μM Na$_3$VO$_4$, 50 μg/ml aprotinin, 50 μg/ml leupeptin, 10% glycerol, and 1% Nonidet P-40). Lysates were centrifuged at 13,000 × g for 15 min, and the supernatants were incubated with anti-IRS-1, anti-IRS-2, or anti-HA antibody for 1 h at 4 °C. Immune complexes were captured with protein A-agarose beads (Invitrogen) and washed three times with lysate buffer A (18).

PI3K Activity Assay—IRS-1-associated PI3K activity was determined by incorporation of [^{32}P]phosphate into phosphatidylinositol using anti-IRS-1 immune complexes. Immune complexes were washed successively with phosphate-buffered saline containing 1% Nonidet P-40 and 100 μM Na$_3$VO$_4$; 10 mM Tris-HCl (pH 7.5) containing 500 mM LiCl and 100 μM Na$_3$VO$_4$; and 100 mM Tris-HCl (pH 7.5) containing 100 mM NaCl, 1 mM EDTA, and 100 μM Na$_3$VO$_4$. The washed immune complexes were resuspended in 50 μl of 10 mM Tris-HCl (pH 7.5) containing 100 mM NaCl and 1 mM EDTA and combined with 10 μl of 100 mM MgCl$_2$ and 10 μl of 2 μg/μl phosphatidylinositol (Avanti Polar Lipids, Inc.) that had been sonicated in 10 mM Tris-HCl (pH 7.5) containing 1 mM EGTA. The assay was initiated by addition of 5 μl of [γ-^{32}P]ATP solution (0.88 mM ATP containing 30 μCi of [γ-^{32}P]ATP and 20 mM MgCl$_2$). The

reaction proceeded for 10 min at room temperature and was terminated by addition of 20 μl of 8 N HCl and 160 μl of CHCl$_3$/methanol (1:1). The samples were vortexed and centrifuged. The lower organic phase was removed and applied to silica gel thin-layer chromatography plates (Merck). The plates were developed in CHCl$_3$/CH$_3$OH/H$_2$O/NH$_4$OH (60:47:11.3:2), dried, and visualized by autoradiography (18).

Akt Activity Assay—Akt activity was measured in anti-HA immune complexes obtained from CHO/IR/IRS-1/HA-Akt cells (18). Immune complexes were washed successively with lysate buffer A, lysate buffer A containing 0.5 M NaCl, and kinase buffer (20 mM HEPES (pH 7.4), 10 mM MgCl$_2$, and 10 mM MnCl$_2$). The reaction was started by addition of 40 μl of kinase buffer containing 50 μM [γ-^{32}P]ATP, 1 mM DTT, and 100 μM Akt substrate peptide (RPRAATF, found in SGK; Upstate) and incubated at room temperature for 20 min. 10 μl of 0.5 M EDTA was added to stop the reaction, and 20-μl aliquots were spotted on P-81 filter papers. The papers were washed five times with 1% phosphoric acid and once with acetone, dried, and counted in a Packard 2200 CA scintillation counter.

Partial Purification of MAPK and Assay for MAPK Activity (24)—Cells were washed once with 10 ml of ice-cold phosphate-buffered saline, frozen in liquid nitrogen, and thawed in 1 ml of lysate buffer B (25 mM Tris-HCl (pH 7.5), 25 mM NaCl, and 2 mM EGTA containing 40 mM p-nitrophenyl phosphate, 1 mM DTT, 200 μM phenylmethylsulfonyl fluoride, and 100 μM Na$_3$VO$_4$). Lysates were centrifuged at 30,000 $\times$ g for 15 min. Ethylene glycol was added to the supernatant fraction (10% final concentration), and 0.5 ml was immediately mixed with 150 μl of packed phenyl-Sepharose for 5 min. The suspension was centrifuged briefly, and unbound material was removed. The phenyl-Sepharose was then successively washed with lysate buffer B containing 10% ethylene glycol and lysate buffer B containing 35% ethylene glycol. MAPK was eluted from the phenyl-Sepharose with 200 μl of lysate buffer B containing 60% ethylene glycol and assayed for MAPK activity using myelin basic protein as a substrate. The reaction was initiated with 5 μl of partially purified MAPK in 40 μl of buffer containing 50 mM β-glycerol phosphate, 10 mM magnesium acetate (pH 7.5), 100 μM [γ-^{32}P]ATP, 1 mM DTT, and 10 μg of myelin basic protein and incubated at room temperature for 15 min. The reaction was stopped by addition of 10 μl of stop solution (0.6% HCl containing 1 mM ATP and 1% bovine serum albumin). Aliquots (20 μl) were spotted on P-81 filter papers. The papers were washed with 1% phosphoric acid and acetone, dried, and counted in the Packard 2200 CA scintillation counter (25).

RESULTS

Phosphorylation of IRS-1, Akt, and ERK1/2 in CHO/IR/IRS-1/HA-Akt Cells during Insulin Stimulation—To investigate protein dephosphorylation, we created a model cell line that overexpressed rat IRS-1 and HA-tagged mouse Akt in CHO cells overexpressing the human IR (CHO/IR/IRS-1/HA-Akt cells). Application of insulin rapidly induced phosphorylation of a number of cellular proteins in this cell line, including the β-subunit of the IR, IRS-1, Akt, and ERK1/2 (Fig. 1). Maximum levels of phosphorylation of IRS-1 and the IR β-subunit at tyrosyl residues occurred within 30 s (Fig. 1*A*). Tyrosine phos-
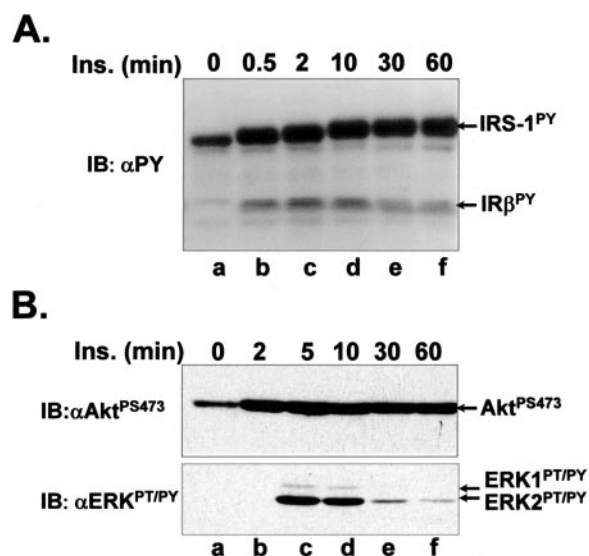

FIGURE 1. **Phosphorylation of IRS-1, Akt, and ERK1/2 during insulin stimulation.** CHO/IR/IRS-1/HA-Akt cells were or were not stimulated with 100 nM insulin (*Ins.*) for the indicated times before being lysed in Laemmli sample buffer containing 0.1 M DTT. Proteins in lysates were separated by SDS-PAGE using 7.5% (*A*) and 10% (*B*) gels and transferred to nitrocellulose membranes. Tyrosine phosphorylation of IRS-1 (IRS-1^{PY}) and the β-subunit of IR (*IRβ^{PY}*; *A*), phosphorylated Akt (*B*, *upper panel*), and phosphorylated ERK1/2 (*B*, *lower panel*) were detected by immunoblot (*IB*) analysis using anti-phosphotyrosine (α*PY*), anti-Akt phospho-Ser^{473} (α*Akt^{PS473}*), and anti-phospho-p44/42 (α*ERK$^{PT/PY}$*) antibodies, respectively. The results are representative of at least two separate experiments.

phorylation of IRS-1 and the IR was observable for at least 60 min (Fig. 1*A*). Akt was serine-phosphorylated in response to insulin (at Ser^{473}); maximum phosphorylation occurred at 2 min after insulin stimulation and remained elevated for 60 min (Fig. 1*B*, *upper panel*). No dephosphorylation of IRS-1 or Akt was observed within the first 30 min of insulin stimulation. ERK1/2 phosphorylation was transient, peaking within 5 min and rapidly fading after 10 min of insulin addition (Fig. 1*B*, *lower panel*). Threonine/tyrosine phosphorylation of ERK1/2 remained elevated above basal levels for 60 min following insulin treatment (Fig. 1*B*, *lower panel*). Changes in the magnitude of phosphorylation of these proteins were not due to changes in protein levels (data not shown).

The intensity of IRS-1, Akt, and ERK1/2 phosphorylation is thought to reflect the degree of their biological activities (11). Therefore, we next examined the insulin-induced IRS-1-associated PI3K activity and Akt and ERK1/2 activation in our model cell system. IRS-1-associated PI3K activity peaked within 10 min after insulin treatment and remained elevated for 1 h (Fig. 2*A*). The same activity profile was observed for insulin-induced activation of Akt (Fig. 2*B*). ERK1/2 activation was transient and peaked at 5 min. ERK1/2 activity decreased by 15 min, but remained elevated above basal levels for 1 h (Fig. 2*C*). The activities of IRS-1-associated PI3K, Akt, and ERK1/2 were consistent with their phosphorylation levels, as shown in Fig. 1.

LY294002 is a potent inhibitor of PI3K (26). When added to the medium before insulin stimulation, no insulin-induced PI3K or Akt activity was observed (data not shown). When cells were stimulated with insulin for 10 min (to activate PI3K), application of LY294002 rapidly abolished PI3K activity (Fig.
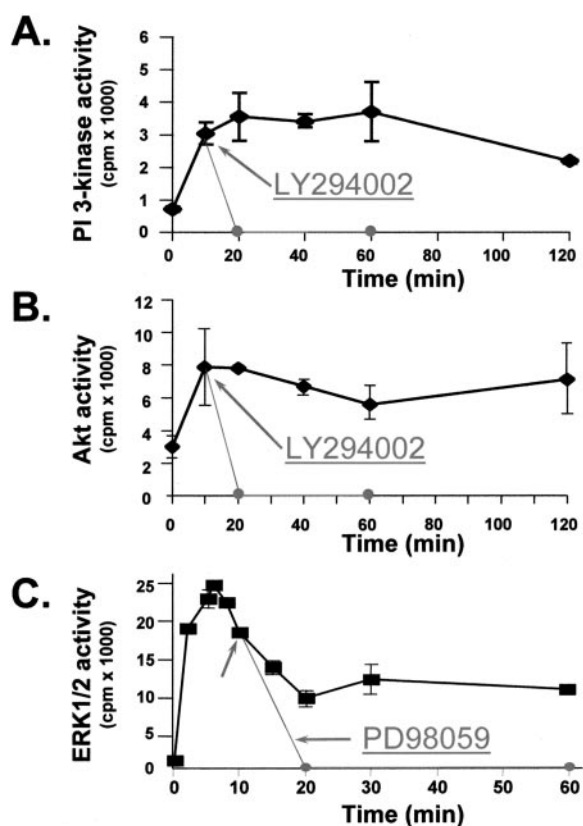
A.

B.

C.

FIGURE 2. **Insulin-induced activation of PI3K, Akt, and ERK1/2.** CHO/IR/IRS-1/HA-Akt cells were or were not stimulated with 100 nm insulin for the indicated times. At 10 min, LY294002 (50 μM) or PD98059 (250 μM) was added to cells as indicated. Cells were lysed in the corresponding lysate buffer. *A*, IRS-1 was immunoprecipitated from cell lysates with anti-IRS-1 antibody, and PI3K activity was measured in the anti-IRS-1 immune complexes. *B*, HA-Akt was immunoprecipitated from cell lysates with anti-HA antibody, and Akt activity was measured in the anti-HA immune complexes using SGK peptide as a substrate. *C*, ERK1/2 were partially purified from lysates using phenyl-Sepharose, and protein kinase activities were measured by an *in vitro* kinase assay using myelin basic protein as a substrate. Data are the means $\pm$ S.D. of triplicate determinations.

2*A*). To our surprise, addition of LY294002 also concurrently abolished Akt activity (Fig. 2*B*). Because PI3K is an upstream kinase for Akt, this suggested that inactivation of an upstream kinase leads to the simultaneous inactivation of its downstream effector. To determine whether the same holds true for the ERK1/2 pathway, we used PD98059, a potent and specific inhibitor of MEK, which is the upstream kinase for ERK1/2 (27). When added to the cells after the initial insulin stimulation, ERK1/2 activity was also completely suppressed (Fig. 2*C*). Together, these results support the existence of a common mechanism operating to decrease Akt and ERK1/2 activities following inactivation of their corresponding upstream kinases.

Dephosphorylation of Akt—Phosphorylation of Akt at Ser[473] or ERK1/2 at Thr[202]/Tyr[204] has been shown to correlate with kinase activity and is considered to be a marker for kinase activation (28–30). Complete loss of Akt and ERK1/2 activities immediately following inhibition of their corresponding upstream kinases prompted us to further examine their dephosphorylation. To measure the dephosphorylation rate of phosphorylated Akt *in vivo*, cells were stimulated with insulin for 10 min to trigger maximum phosphorylation of Akt (Figs. 1

and 3*A*, *lane i*); subsequently, LY294002 was added to the medium to inhibit PI3K. The levels of phosphorylation of Akt were determined by Western blot analysis using a specific antibody against Akt phospho-Ser[473] to assess the dephosphorylation rate. The insulin-induced phosphorylation of Akt was completely abolished 20 min after addition of LY294002 (Fig. 3*A*, *lane f versus lanes i* and *k*). In control cells, Akt Ser[473] remained phosphorylated during 30 min of insulin stimulation (Figs. 1*B* and 3*A*, *lanes i–k*), and preincubation of cells with LY294002 for 10 min prevented the insulin-induced Ser[473] phosphorylation of Akt (Fig. 3*A*, *lane d*).

We also determined the rate of dephosphorylation of Akt following inhibition of PI3K activity with LY294002. Significant dephosphorylation (by 80%) was detected at 2.5 min, and the effect was nearly complete by 5 min (Fig. 3*B*, *lanes b–e versus lanes f–h*). Taking the diffusion rate of LY294002 across the cell membrane into consideration, dephosphorylation of Akt was notably expeditious.

We next determined whether protein phosphatase (PP)-2A and PP1 are responsible for Akt dephosphorylation by using calyculin A, a specific inhibitor of PP2A and PP1 (31). Calyculin A failed to prevent the dephosphorylation of Akt (Fig. 3*A*, *lane h versus lanes f, i*, and *k*) when cells were exposed to the PI3K inhibitor after maximum insulin stimulation. This raises the possibility that other phosphatases dephosphorylate Akt under insulin-stimulated conditions. Interestingly, adding calyculin A in the absence of ligand slightly increased the basal phosphorylation of Akt at Ser[473] (Fig. 3*A*, *lane a versus lane c*), indicating that calyculin A inhibited PP2A and PP1 in the unstimulated condition and thus may participate in dephosphorylation of Akt in basal states.

The experiments above were conducted in a transformed cell line designed to overexpress the IR, IRS-1, and Akt; to determine whether the rapid dephosphorylation following addition of LY294002 occurs in more physiologically relevant systems, we carried out similar experiments in the hepatocyte cell line H2.35 and in freshly isolated mouse primary hepatocytes. H2.35 is an epithelium-like cell line derived from mouse primary hepatocytes infected with a temperature-sensitive mutant of the SV40 virus; it maintains some hepatocyte behavior, including synthesis of albumin (19, 20, 32, 33). Consistent with the results obtained with CHO/IR/IRS-1/HA-Akt cells, rapid dephosphorylation of phosphorylated Akt was observed following inhibition of PI3K in both H2.35 cells (Fig. 3*C*, *upper and middle panels*, *lanes a–d versus lanes i–l*) and primary hepatocytes (Fig. 3*C*, *lower panel*, *lanes a–d versus lanes i–l*). Moreover, this effect was seen even with 1 nm insulin (Fig. 3*C*, *lane b versus lane j*).

Dephosphorylation of ERK1/2—To determine whether the rapid dephosphorylation of proteins is specific to Akt or whether it is a general phenomenon, we examined the dephosphorylation of ERK1/2 in cells after inhibition of MEK with PD98059. The insulin-induced phosphorylation of ERK1/2 was completely abolished 20 min after addition of PD98059 (Fig. 4*A*, *lane f versus lanes i–k*). In contrast, ERK1/2 remained phosphorylated during 30 min of insulin treatment (Fig. 4*A*, *lanes i–k*).
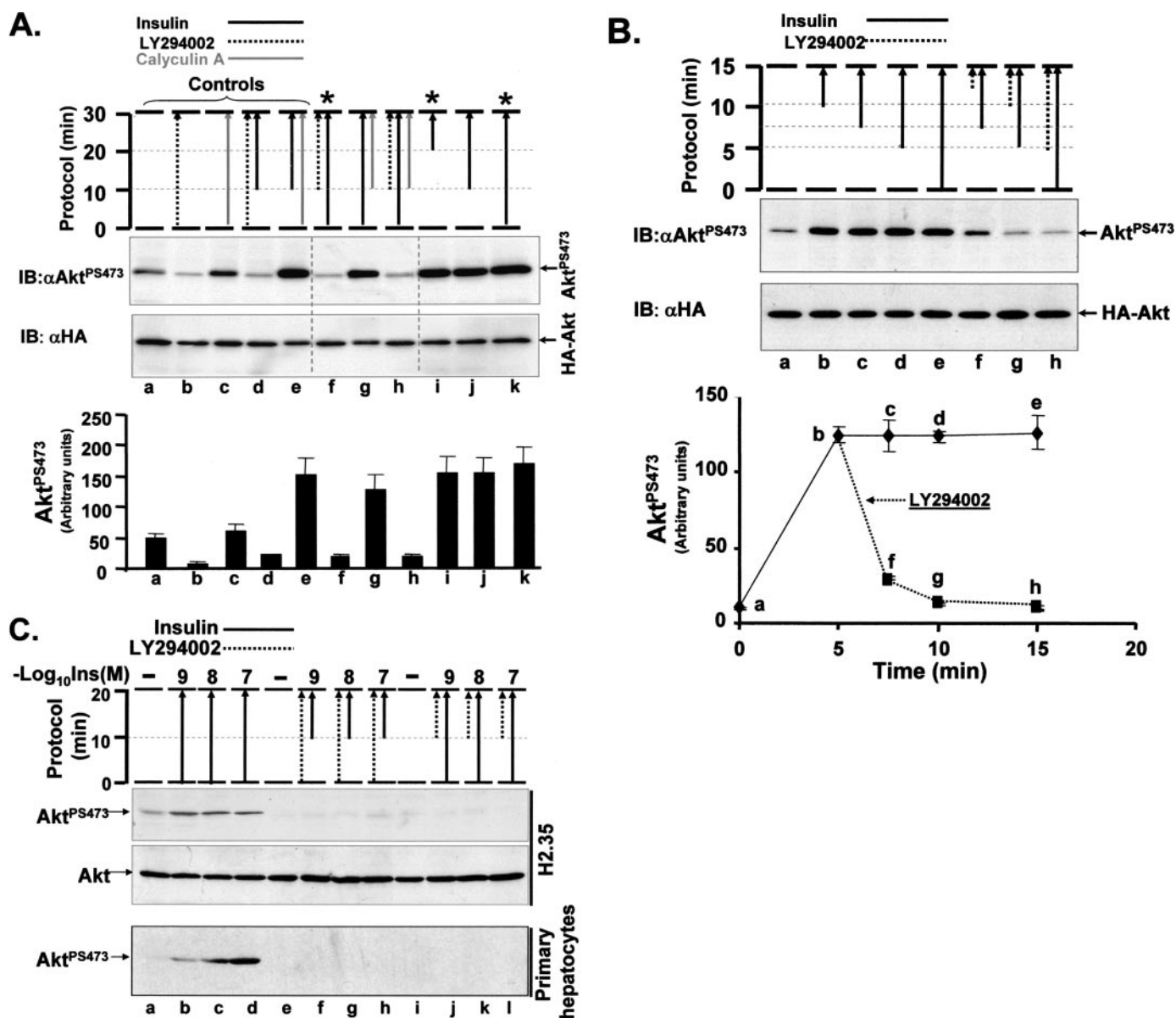
FIGURE 3. **Phosphorylation and dephosphorylation of Akt.** *A*, CHO/IR/IRS-1/HA-Akt cells were left untreated or were exposed to calyculin A (*gray arrows*), LY294002 (*dotted arrows*), or insulin (*black arrows*) as indicated in the protocol before being lysed in Laemmli sample buffer containing 0.1 M DTT. *IB*, immunoblot. *B*, CHO/IR/IRS-1/HA-Akt cells were exposed to 100 nM insulin (*black arrows*), and 50 μM LY294002 (*dotted arrows*) was added as indicated in the protocol. Cells were lysed in Laemmli sample buffer containing 0.1 M DTT. *C*, H2.35 cells and primary hepatocytes were left untreated or were exposed to LY294002 (*dotted arrows*) or various doses of insulin (*Ins*) in the protocol before being lysed in Laemmli sample buffer containing 0.1 M DTT. Proteins in lysates from *A–C* were separated by 10% SDS-PAGE and transferred to nitrocellulose membranes. Phosphorylated Akt and Akt proteins were detected with anti-Akt phospho-Ser[473] antibody (α*Akt*[PS473]) and anti-HA or anti-Akt antibody, respectively. The results are representative of multiple experiments. Data shown in *A* and *B* are the means ± S.D. of triple determinations.

We determined the dephosphorylation rate of ERK1/2 following inhibition of MEK with PD98059. As with Akt, significant dephosphorylation of ERK1/2 (by >80%) occurred within 2.5 min (Fig. 4*B*, *lane f versus lanes b* and *c*) and was complete within 10 min of PD98059 application (*lane h versus lane e*). It should be pointed out that the kinetics of dephosphorylation of ERK1/2 surprisingly resembles that of Akt (Fig. 3*B*).

Calyculin A was introduced to determine the contribution of PP2A/PP1 in dephosphorylation of ERK1/2. Calyculin A only partially prevented the effect of PD98059 on ERK1/2 dephosphorylation (Fig. 4*A*, *lane h versus lanes f* and *i*). In contrast to Akt, basal ERK1/2 phosphorylation was not affected by calyculin A (Fig. 4*A*, *lane a versus lane c*).

Dephosphorylation of ERK1/2 was also examined in H2.35 cells and mouse primary hepatocytes. Consistent with the results obtained with CHO/IR/IRS-1/HA-Akt cells, rapid dephosphorylation of ERK1/2 occurred after MEK was inhibited in both H2.35 cells and primary hepatocytes (Fig. 4*C*, *lanes a–d versus lanes i–l*). As with Akt, this effect was also seen with 1 nM insulin (Fig. 4*C*, *lane b versus lane j*).

Dephosphorylation of IRS-1—Finally, we examined the levels of insulin-induced tyrosyl phosphorylation of IRS-1 following inhibition of IR tyrosine kinase with HNMPA-(AM)₃, a relatively specific inhibitor of IR tyrosine kinase activity (34, 35). Preincubation of cells with HNMPA-(AM)₃ for 10 min prevented the insulin-induced tyrosyl phosphorylation of both
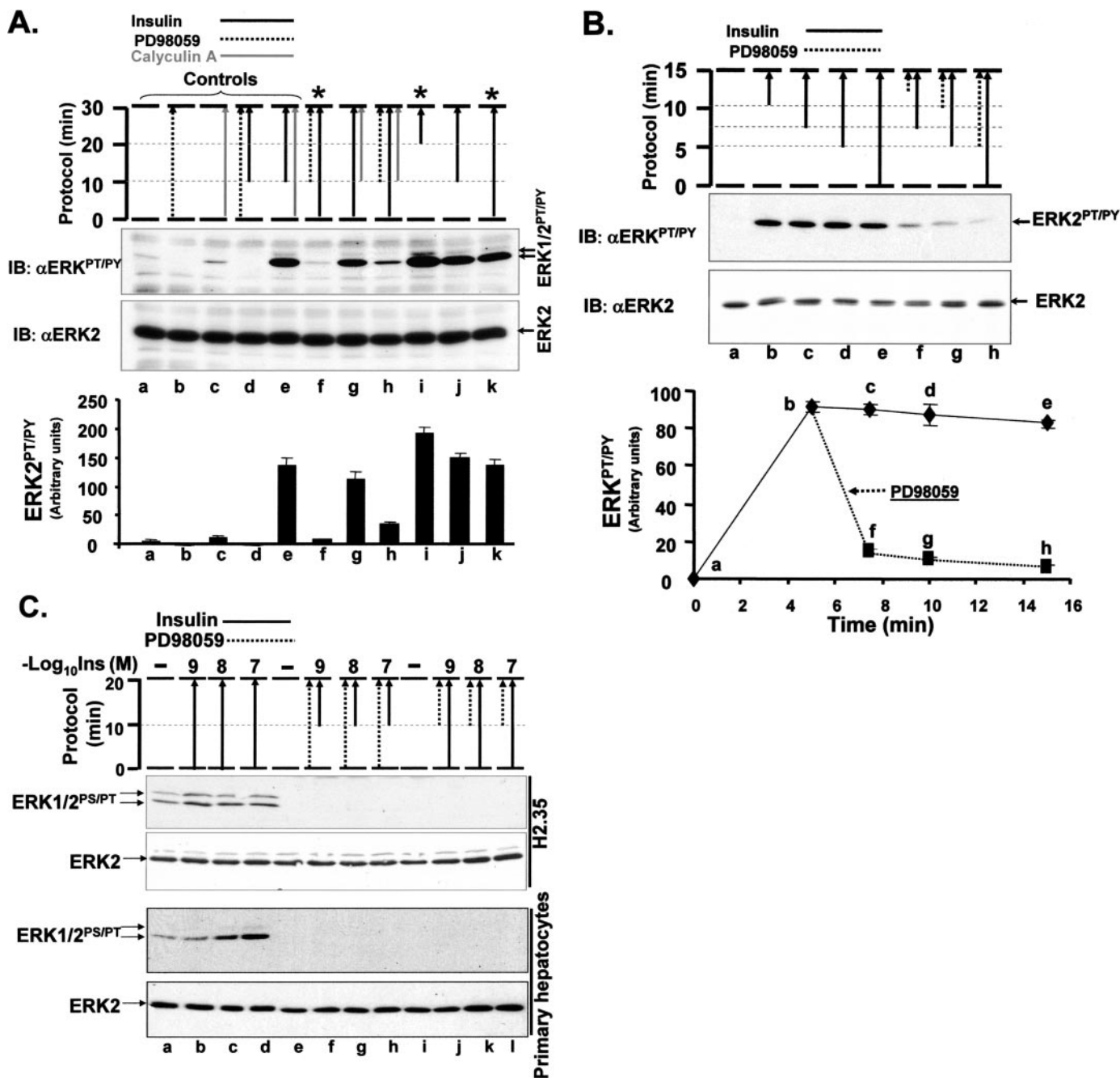
Dephosphorylation by Default

A.

B.

C.

FIGURE 4. **Phosphorylation and dephosphorylation of ERK1/2.** *A*, CHO/IR/IRS-1/HA-Akt cells were exposed to various agents as indicated in the protocol before being lysed in Laemmli sample buffer containing 0.1 M DTT. *B*, CHO/IR/IRS-1/HA-Akt cells were exposed to 100 nM insulin (*black arrows*), and 250 μM PD98059 (*dotted arrows*) was added as indicated in the protocol. Incubation was terminated by addition of Laemmli sample buffer containing 0.1 M DTT. *C*, H2.35 cells and primary hepatocytes were left untreated or were exposed to PD98059 (*dotted arrows*) or various doses of insulin (*Ins*; *black arrows*) as indicated in the protocol before being lysed in Laemmli sample buffer containing 0.1 M DTT. Proteins in lysates from *A–C* were separated by 10% SDS-PAGE and transferred to nitrocellulose membranes. Phosphorylated ERK1/2 (*upper panel*) and ERK2 (*lower panel*) proteins were immunoblotted (*IB*) with anti-phospho-ERK (αERK$^{PT/PY}$) and anti-ERK2 antibodies, respectively. The results are representative of multiple experiments. Data shown in *A* and *B* are the means $\pm$ S.D. of triple determinations.

IRS-1 and the IR (Fig. 5, *lane d versus lane i*), suggesting that HNMPA-(AM)$_3$ can inhibit IR tyrosine kinase activity in our cell line. When maximum tyrosyl phosphorylation of IRS-1 was first achieved by 10 min of insulin stimulation, followed by inhibition of IR tyrosine kinase activity with HNMPA-(AM)$_3$, the levels of tyrosyl-phosphorylated IRS-1 significantly decreased within 10 min (by >80%) (Fig. 5*A*, *lane i versus lanes f* and *j*). To determine whether this effect was due to protein-tyrosine

phosphatase activity, we treated cells with vanadate, a tyrosine phosphatase inhibitor that has been shown to prevent dephosphorylation of IRS-1 and the IR (36). Preincubation of cells with vanadate (without HNMPA-(AM)$_3$) slightly increased the insulin-induced tyrosyl phosphorylation of both IRS-1 and the β-subunit of the IR (Fig. 5*A*, *lane e versus lane i*). When given to cells exposed to insulin and HNMPA-(AM)$_3$, vanadate prevented the decreased tyrosyl phosphorylation of IRS-1 previ-
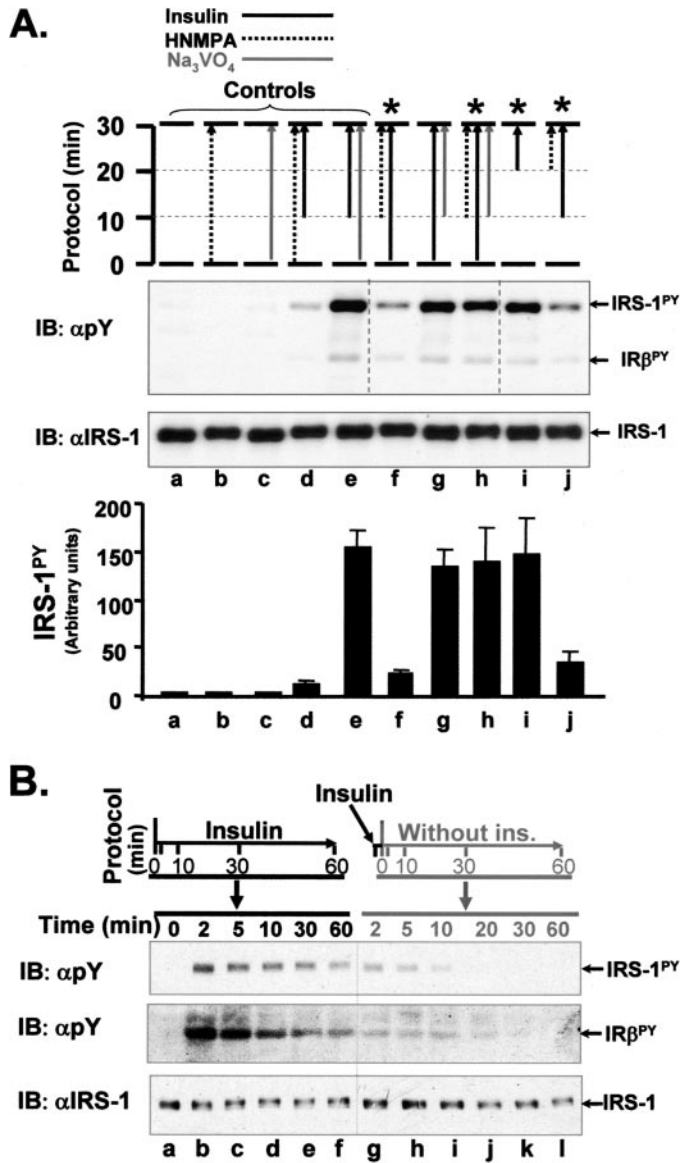
A.

B.

FIGURE 5. **Phosphorylation and dephosphorylation of IRS-1 and the IR.** *A*, CHO/IR/IRS-1/HA-Akt cells were exposed to various agents as indicated in the protocol before being lysed in Laemmli sample buffer containing 0.1 M DTT. *B, lanes a-f*, CHO/IR/IRS-1/HA-Akt cells were exposed to 100 nM insulin for the indicated times in fasting medium (see "Experimental Procedures"); *lanes g-l*, cells were exposed to 100 nM insulin for 2 min, washed twice briefly with phosphate-buffered saline, and incubated in fasting medium without insulin (*ins.*). Cells were lysed at the indicated times in Laemmli sample buffer containing 0.1 M DTT. Proteins in lysates from *A* and *B* were separated by 7% SDS-PAGE and transferred to nitrocellulose membranes. Phosphorylated IRS-1 (*IRS-1^{PY}*; *upper panel*), the phosphorylated β-subunit of IR (*IRβ^{PY}*; *middle panel*), and IRS-1 protein (*lower panel*) were immunoblotted (*IB*) with anti-phosphotyrosine (*αpY*) and anti-IRS-1 antibodies as indicated. The results are representative of multiple experiments. Data shown in *A* are the means ± S.D. of triple determinations.

FIGURE 6. **Phosphorylation and dephosphorylation of IRS-1/2, Akt, and ERK1/2 after inactivation of IR tyrosine kinase in the H2.35 cell line.** H2.35 cells were left untreated or were exposed insulin (*black arrows*) or HNMPA-(AM)$_3$ (*dotted arrows*) before or after insulin stimulation as indicated in the protocol. At the end of 30 min of incubation, cells were lysed in lysate buffer A. IRS-1 and IRS-2 were immunoprecipitated by anti-IRS-1 and anti-IRS-2 antibodies, respectively. Proteins in immune complexes and lysates were separated by 7% SDS-PAGE (for analyzing IRS-1/2) or 10% SDS-PAGE (for analyzing Akt or ERK) and transferred to nitrocellulose membranes. Phosphorylated IRS-1 (*IRS-1^{PY}*) and IRS-2 (*IRS-2^{PY}*) (*first* and *third panels*, respectively) were immunoblotted with anti-phosphotyrosine antibody. IRS-1 and IRS-2 proteins (*second* and *fourth panels*, respectively) were immunoblotted with anti-IRS-1 and anti-IRS-2 antibodies, respectively. Phosphorylated Akt (*Akt^{PS473}*) (*fifth panel*) and Akt (*sixth panel*) proteins were detected with anti-Akt phospho-Ser^{473} and anti-Akt antibodies, respectively. Phosphorylated ERK1/2 (*ERK1/2$^{PS/PT}$*) (*seventh panel*) and ERK2 (*eight panel*) proteins were immunoblotted with anti-phospho-ERK and anti-ERK2 antibodies, respectively.

ously observed upon HNMPA-(AM)$_3$ treatment (Fig. 5*A, lane h versus lanes f, i*, and *j*).

Circulating insulin has a short half-life and is quickly cleared by the liver and kidneys in whole animals (37–39). To mimic the *in vivo* clearance of insulin and its effects on immediate downstream signaling, insulin was removed from the cell culture medium after brief introduction (2 min). Significant dephosphorylation of IRS-1 was detected within 2 min of insulin
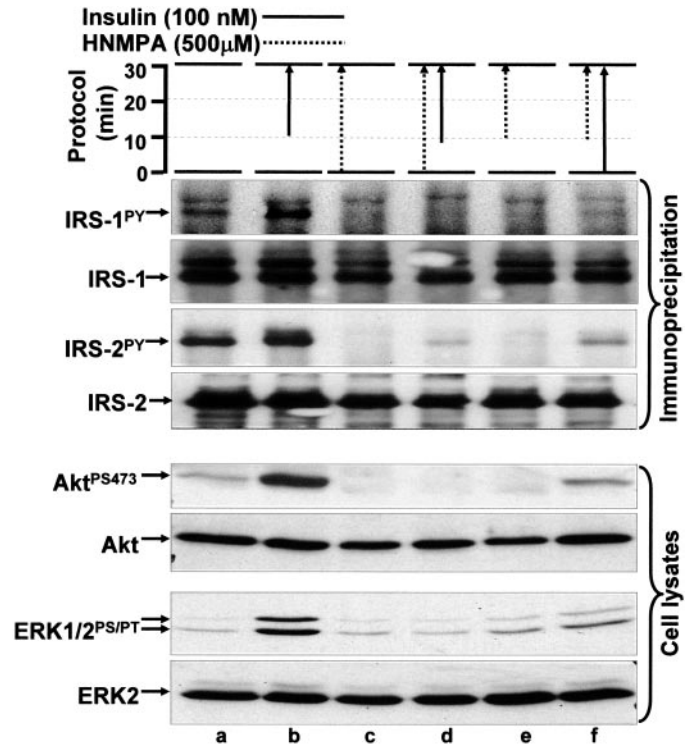
removal, presumably through inactivation of the IR via internalization into endosomes (Fig. 5*B, lanes g-l versus lanes b-f*). Within 20 min of removal of insulin from the medium, neither the IR nor IRS-1 displayed any significant tyrosyl phosphorylation (Fig. 5*B, lanes j–l versus lanes d–f*).

Dephosphorylation of IRS-1 and IRS-2 was also examined in H2.35 cells. As expected, both IRS-1 and IRS-2 were dephosphorylated much more rapidly after IR tyrosine kinase was inhibited by HNMPA-(AM)$_3$ (Fig. 6, *upper four panels, lanes a* and *b versus lanes e* and *f*). More interestingly, the dephosphorylation of IRS-1/IRS-2 translated into the dephosphorylation of Akt and ERK1/2 (Fig. 6, *lower four panels, lanes a* and *b versus lanes e* and *f*) as if PI3K or MEK were inhibited (Figs. 3*A* and 4*A, lane k versus lane f*), respectively. Thus, inactivation of the upstream kinase accelerated the dephosphorylation rate not only of immediate downstream proteins, but also of proteins farther downstream in the signaling cascade.

DISCUSSION

Protein dephosphorylation in cultured cells has often been monitored in the presence of stimuli, which reflects the net

Dephosphorylation by Default

balance between phosphorylation and dephosphorylation (40, 41). In addition, the role of phosphatases has been assessed indirectly in experiments conducted in the presence of phosphatase inhibitors and stimuli or in genetically engineered cells overexpressing phosphatases (6, 42–45). However, these approaches do not allow the contribution of constitutively active phosphatases to be determined. To directly study phosphatases in intact living cells in the presence of insulin, we initiated maximum protein phosphorylation by stimulating CHO/IR/IRS-1/HA-Akt cells, H2.35 cells, or mouse primary hepatocytes with insulin and then measured the dephosphorylation (over time) of three downstream effectors of IR signaling in the absence of their corresponding upstream protein kinase activities. Under such conditions, we found that dephosphorylation of IRS-1/2, Akt, and ERK1/2 occurred almost immediately. Rapid dephosphorylation was also evident following displacement of the original signal either by removing insulin or by inhibiting IR tyrosine kinase activity. Our findings support the hypothesis that cellular proteins are dephosphorylated by default, presumably via constitutively active phosphatases. This default dephosphorylation keeps cellular proteins in their dephosphorylated state in the absence of upstream protein kinase activity.

IRS-1/2, Akt, and ERK1/2 are phosphorylated by different upstream protein kinases during insulin stimulation (11). IRS-1/2 is a direct substrate for the intrinsic activity of the IR tyrosine kinase and is phosphorylated at tyrosine residues upon insulin binding to its receptor, whereas Akt is a substrate for PI3K-dependent kinases. ERK1/2, a substrate for MEK, is phosphorylated (by MEK) at both threonine and tyrosine residues upon insulin treatment. We confirmed that the kinetics of IRS-1/2, Akt, and ERK1/2 phosphorylation following administration of insulin are very different. The phosphorylation of IRS-1/2 and Akt was more sustained, whereas that of ERK1/2 was rather transient. The different kinetics of phosphorylation of these proteins reflect the presence of different upstream kinase and phosphatase activities during insulin stimulation.

The major finding of this study is that, when insulin-induced upstream kinases are inactivated, downstream phosphoproteins immediately return to their unphosphorylated states. Inactivating the upstream kinases revealed that the dephosphorylation rates of IRS-1/2, Akt, and ERK1/2 were not only much faster (within 5 min), but also appeared to follow similar kinetics. These data allow us to speculate that cellular proteins are constitutively dephosphorylated via a common default mechanism, most likely mediated by constitutively active phosphatases. Based on this model, upstream kinases activated by insulin overcome the default mechanism, leading to protein phosphorylation.

It should be stressed that our proposed model of dephosphorylation by default does not exclude or minimize the role of specific regulated phosphatases in dephosphorylation of proteins. It is well known that specific phosphatases exhibiting strict substrate preference participate in the regulation of protein dephosphorylation. Targeted dephosphorylation via specific phosphatases has been reported not only in phosphotyrosine phosphatases, but also in serine/threonine phosphatases (3, 7). Phosphotyrosine phosphatase-1B has been implicated in

dephosphorylation of the IR and IRS-1 at tyrosine residues (46, 47). MAPK phosphatases specifically dephosphorylate MAPKs (8) and are activated only when they bind to the activated phosphorylated form of MAPK, suggesting a specific kinase-induced regulation (9, 10). The pleckstrin homology domain/leucine-rich repeat protein phosphatase PHLPP has been reported to dephosphorylate Ser^{473} in Akt (48).

Although these aforementioned studies provide an excellent explanation for the kinetics of dephosphorylation during stimulation, insulin-induced phosphatase activities cannot fully explain the rapid and uniform dephosphorylation kinetics we observed in the absence of upstream kinase activity. On the basis of the dephosphorylation kinetics, we propose that regulated phosphatases participate in fine-tuning protein dephosphorylation in the presence of upstream kinase activities. However, upon kinase inactivation, the default mechanism would predominate and return the members of the pathway to a basal state. This could explain why different phosphoproteins have distinct dephosphorylation kinetics in the presence of upstream kinase activity (because of the activation of specific phosphatases), but similar dephosphorylation kinetics following inactivation of these kinases. Furthermore, on the basis of our results, we predict that the dephosphorylation capacity of the default mechanism is far greater than that of regulated phosphatases.

In support of our model, the dephosphorylation of ERK1 has been directly examined *in vitro* by a dephosphorylation assay using phosphorylated ERK1 as a substrate and cell extracts (prepared from unstimulated or stimulated cells) as a source of phosphatase. The extracts prepared from unstimulated cells were found to contain maximum phosphatase activity toward phosphorylated ERK1, suggesting that constitutively active phosphatases are the predominant enzymes implicated in the dephosphorylation of ERK1/2 (49).

The identity of the phosphatases involved in the proposed default dephosphorylation mechanism remains unclear. The serine/threonine protein phosphatase family was initially restricted to four biochemically distinct entities: PP1, PP2A, PP2B/calcineurin (a Ca^{2+}-dependent enzyme), and PP2C (a Mg^{2+}-dependent enzyme) (50, 51). Among the numerous members, PP1 and PP2A are considered to be the principal enzymes because of their ubiquitous expression and broad specificity (50). Okadaic acid, a potent inhibitor of PP1 and PP2A, is known to induce serine/threonine hyperphosphorylation of many cellular proteins, including IRS-1 (6, 52–54, 56). These observations provide additional evidence supporting the existence of constitutively active phosphatases that maintain cellular proteins in an unphosphorylated state.

PP2A has been proposed to dephosphorylate Akt and ERK1/2 and to negatively regulate their function based on experiments in which alteration of PP2A activity in cells led to changes in insulin-induced Akt and ERK1/2 phosphorylation (57–59). On the other hand, PP2A was found in another study to positively regulate ERK activity and phosphorylation (60); the reason for this discrepancy is unknown. Because the dephosphorylation rates of Akt and ERK1/2 were not directly measured in those studies, it is unclear whether changes in the phosphorylation of Akt and ERK1/2 were due to direct dephos-

phorylation by PP2A or were an indirect effect (by another phosphatase/phosphatases).

In contrast to the above experiments, our current approach offers direct measurement of the dephosphorylation rate of the aforementioned proteins in living cells. Calyculin A, a specific inhibitor of PP1 and PP2A, failed to inhibit the dephosphorylation of Akt and ERK1/2, suggesting that PP1 and PP2A do not play a major role in the default dephosphorylation of Akt and ERK1/2, at least under our experimental conditions.

Although constitutive dephosphorylation will likely have an impact on the duration of a phosphorylation-induced signal, our data do not directly address how the upstream kinases for Akt and ERK1/2 are inactivated. Additional mechanisms for signal dampening exist, *e.g.* phosphoproteins can be targeted for translocation or degradation. As an example, serine phosphorylation is recognized as a signal for ubiquitin/proteasome-mediated degradation (55, 61). Additionally, the internalization of activated IRs into endosomes can result in their recycling back to the plasma membrane, but as inactive tyrosine kinases (39). Consistent with this latter possibility, we have shown that autophosphorylation of the IR was greatly reduced either by removal of insulin from the medium or by addition of a specific tyrosine kinase inhibitor, leading to rapid dephosphorylation of IRS-1/2, Akt, and ERK1/2.

The results from these experiments are consistent with our model of dephosphorylation by default and integrate to provide a potential explanation of how IR signaling is turned off *in vivo*. Insulin secreted from the pancreas in response to the elevation of blood glucose is quickly cleared by the liver and kidneys after exerting its hypoglycemic effects by inducing signaling in insulin-sensitive tissues (37–39). Shortly after binding insulin, IR tyrosine kinase is then internalized and inactivated. This results in rapid dephosphorylation of the IR, IRS-1/2, Akt, ERK1/2, and other molecules in the signaling chain by the default dephosphorylation mechanism. Under normal (healthy) conditions, this will have occurred in time for sufficient (insulin) signaling to occur in insulin-responsive tissues, returning the organism to a euglycemic state.

In summary, our data suggest that the phosphorylation state of downstream effectors of IR signaling cascades is regulated by a default mechanism that maintains proteins in an unphosphorylated state when ligand/stimulation is lacking. This mechanism dephosphorylates phosphoserine, phosphothreonine, and phosphotyrosine residues in multiple proteins and may regulate phosphoprotein signal transduction by setting the thresholds for protein phosphorylation by an upstream kinase. Signaling by net phosphorylation would thus occur only after the kinase activity surpasses the threshold set by the constitutively active phosphatases. Then, upon cessation of cellular stimulation, the amount of phosphorylation would rapidly decrease consequent to the activity of said phosphatases. On the basis of this model, one could envision that any perturbation of this dephosphorylation activity, such as nutritional status, might shift the preset threshold. This would lead to alterations in the efficacy of insulin-induced kinase activity with respect to downstream effectors, ultimately affecting the physiological manifestations of insulin signaling.

REFERENCES

1. Cohen, P. T. (1997) *Trends Biochem. Sci.* **22,** 245–251
2. Mumby, M. C., and Walter, G. (1993) *Physiol. Rev.* **73,** 673–699
3. Alonso, A., Sasin, J., Bottini, N., Friedberg, I., Friedberg, I., Osterman, A., Godzik, A., Hunter, T., Dixon, J., and Mustelin, T. (2004) *Cell* **117,** 699–711
4. Gee, C. E., and Mansuy, I. M. (2005) *CMLS Cell. Mol. Life Sci.* **62,** 1120–1130
5. Gum, R. J., Gaede, L. L., Koterski, S. L., Heindel, M., Clampit, J. E., Zinker, B. A., Trevillyan, J. M., Ulrich, R. G., Jirousek, M. R., and Rondinone, C. M. (2003) *Diabetes* **52,** 21–28
6. Haystead, T. A., Sim, A. T., Carling, D., Honnor, R. C., Tsukitani, Y., Cohen, P., and Hardie, D. G. (1989) *Nature* **337,** 78–81
7. Gallego, M., and Virshup, D. M. (2005) *Curr. Opin. Cell Biol.* **17,** 197–202
8. Ducruet, A. P., Vogt, A., Wipf, P., and Lazo, J. S. (2005) *Annu. Rev. Pharmacol. Toxicol.* **45,** 725–750
9. Keyse, S. M. (2000) *Curr. Opin. Cell Biol.* **12,** 186–192
10. Farooq, A., and Zhou, M. M. (2004) *Cell. Signal.* **16,** 769–779
11. White, M. F. (2002) *Am. J. Physiol.* **283,** E413–E422
12. Pullen, N., Dennis, P. B., Andjelkovic, M., Dufner, A., Kozma, S. C., Hemmings, B. A., and Thomas, G. (1998) *Science* **279,** 707–710
13. Alessi, D. R., Kozlowski, M. T., Weng, Q. P., Morrice, N., and Avruch, J. (1998) *Curr. Biol.* **8,** 69–81
14. Alessi, D. R., James, S. R., Downes, C. P., Holmes, A. B., Gaffney, P. R., Reese, C. B., and Cohen, P. (1997) *Curr. Biol.* **7,** 261–269
15. Myers, M. G., Jr., Wang, L. M., Sun, X. J., Zhang, Y., Yenush, L., Schlessinger, J., Pierce, J. H., and White, M. F. (1994) *Mol. Cell. Biol.* **14,** 3577–3587
16. Yamauchi, K., and Pessin, J. E. (1994) *Mol. Cell. Biol.* **14,** 4427–4434
17. Robinson, M. J., and Cobb, M. H. (1997) *Curr. Opin. Cell Biol.* **9,** 180–186
18. Zhande, R., Mitchell, J. J., Wu, J., and Sun, X. J. (2002) *Mol. Cell. Biol.* **22,** 1016–1026
19. Liu, J. K., DiPersio, C. M., and Zaret, K. S. (1991) *Mol. Cell. Biol.* **11,** 773–784
20. Zaret, K. S., DiPersio, C. M., Jackson, D. A., Montigny, W. J., and Weinstat, D. L. (1988) *Proc. Natl. Acad. Sci. U. S. A.* **85,** 9076–9080
21. Sun, X. J., Goldberg, J. L., Qiao, L. Y., and Mitchell, J. J. (1999) *Diabetes* **48,** 1359–1364
22. Klaunig, J. E., Goldblatt, P. J., Hinton, D. E., Lipsky, M. M., and Trump, B. F. (1981) *In Vitro* **17,** 926–934
23. Klaunig, J. E., Goldblatt, P. J., Hinton, D. E., Lipsky, M. M., Chacko, J., and Trump, B. F. (1981) *In Vitro* **17,** 913–925
24. Anderson, N. G., Kilgour, E., and Sturgill, T. W. (1991) *J. Biol. Chem.* **266,** 10131–10135
25. Ray, L. B., and Sturgill, T. W. (1988) *J. Biol. Chem.* **263,** 12721–12727
26. Vlahos, C. J., Matter, W. F., Hui, K. Y., and Brown, R. F. (1994) *J. Biol. Chem.* **269,** 5241–5248
27. Waters, S. B., Holt, K. H., Ross, S. E., Syu, L. J., Guan, K. L., Saltiel, A. R., Koretzky, G. A., and Pessin, J. E. (1995) *J. Biol. Chem.* **270,** 20883–20886
28. Alessi, D. R., Andjelkovic, M., Caudwell, B., Cron, P., Morrice, N., Cohen, P., and Hemmings, B. A. (1996) *EMBO J.* **15,** 6541–6551
29. Datta, S. R., Brunet, A., and Greenberg, M. E. (1999) *Genes Dev.* **13,** 2905–2927
30. Payne, D. M., Rossomando, A. J., Martino, P. A., Erickson, A. K., Her, J. H., Shabanowitz, J., Hunt, D. F., Weber, M. J., and Sturgill, T. W. (1991) *EMBO J.* **10,** 885–892
31. Ishihara, H., Martin, B. L., Brautigan, D. L., Karaki, H., Ozaki, H., Kato, Y., Fusetani, N., Watabe, S., Hashimoto, K., Uemura, D., and Hartshorne, D. J. (1989) *Biochem. Biophys. Res. Commun.* **159,** 871–877
32. Zaret, K. S., and Stevens, K. A. (1990) *Mol. Cell. Biol.* **10,** 4582–4589
33. DiPersio, C. M., Jackson, D. A., and Zaret, K. S. (1991) *Mol. Cell. Biol.* **11,** 4405–4414

34. Baltensperger, K., Lewis, R. E., Woon, C. W., Vissavajjhala, A. H., Ross, A. H., and Czech, M. P. (1992) *Proc. Natl. Acad. Sci. U. S. A.* **89,** 7885–7889
35. Saperstein, R., Vicario, P. P., Strout, H. V., Brady, E. J., Slater, E. E., Greenlee, W. J., Ondeyka, D. L., Patchett, A. A., and Hangauer, D. G. (1989) *Biochemistry* **28,** 5694–5701
36. Mooney, R. A., and Anderson, D. L. (1989) *J. Biol. Chem.* **264,** 6850–6857
37. Valera Mora, M. E., Scarfone, A., Calvani, M., Greco, A. V., and Mingrone, G. (2003) *J. Am. Coll. Nutr.* **22,** 487–493
38. Misbin, R. I., Merimee, T. J., and Lowenstein, J. M. (1976) *Am. J. Physiol.* **230,** 171–177
39. Di Guglielmo, G. M., Drake, P. G., Baass, P. C., Authier, F., Posner, B. I., and Bergeron, J. J. (1998) *Mol. Cell. Biochem.* **182,** 59–63
40. Miralpeix, M., Sun, X. J., Backer, J. M., Myers, M. G., Jr., Araki, E., and White, M. F. (1992) *Biochemistry* **31,** 9031–9039
41. Sun, X. J., Miralpeix, M., Myers, M. G., Jr., Glasheen, E. M., Backer, J. M., Kahn, C. R., and White, M. F. (1992) *J. Biol. Chem.* **267,** 22662–22672
42. Ahmad, F., Li, P. M., Meyerovitch, J., and Goldstein, B. J. (1995) *J. Biol. Chem.* **270,** 20503–20508
43. Denu, J. M., and Dixon, J. E. (1998) *Curr. Opin. Chem. Biol.* **2,** 633–641
44. Brondello, J. M., Pouyssegur, J., and McKenzie, F. R. (1999) *Science* **286,** 2514–2517
45. Brady, M. J., and Saltiel, A. R. (2001) *Recent Prog. Horm. Res.* **56,** 157–173
46. Goldstein, B. J., Bittner-Kowalczyk, A., White, M. F., and Harbeck, M. (2000) *J. Biol. Chem.* **275,** 4283–4289
47. Venable, C. L., Frevert, E. U., Kim, Y. B., Fischer, B. M., Kamatkar, S., Neel, B. G., and Kahn, B. B. (2000) *J. Biol. Chem.* **275,** 18318–18326
48. Gao, T., Furnari, F., and Newton, A. C. (2005) *Mol. Cell* **18,** 13–24
49. Peraldi, P., Scimeca, J. C., Filloux, C., and Van Obberghen, E. (1993) *Endocrinology* **132,** 2578–2585
50. Wera, S., and Hemmings, B. A. (1995) *Biochem. J.* **311,** 17–29
51. Cohen, P. T. (1993) *Biochem. Soc. Trans.* **21,** 884–888
52. Tanti, J. F., Gremeaux, T., Van Obberghen, E., and Le Marchand-Brustel, Y. (1994) *J. Biol. Chem.* **269,** 6051–6057
53. Haystead, T. A., Weiel, J. E., Litchfield, D. W., Tsukitani, Y., Fischer, E. H., and Krebs, E. G. (1990) *J. Biol. Chem.* **265,** 16571–16580
54. Rondinone, C. M., and Smith, U. (1996) *J. Biol. Chem.* **271,** 18148–18153
55. Nash, P., Tang, X., Orlicky, S., Chen, Q., Gertler, F. B., Mendenhall, M. D., Sicheri, F., Pawson, T., and Tyers, M. (2001) *Nature* **414,** 514–521
56. Luscher, B., Brizuela, L., Beach, D., and Eisenman, R. N. (1991) *EMBO J.* **10,** 865–875
57. Carpenter, G., King, L. E., Jr., and Cohen, S. (1979) *J. Biol. Chem.* **254,** 4884–4891
58. Jadus, M. R., Good, R. W., Crumpacker, D. B., and Yannelli, J. R. (1991) *J. Leukocyte Biol.* **49,** 139–151
59. Van Kanegan, M. J., Adams, D. G., Wadzinski, B. E., and Strack, S. (2005) *J. Biol. Chem.* **280,** 36029–36036
60. Adams, D. G., Coffee, R. L., Jr., Zhang, H., Pelech, S., Strack, S., and Wadzinski, B. E. (2005) *J. Biol. Chem.* **280,** 42644–42654
61. Skowyra, D., Craig, K. L., Tyers, M., Elledge, S. J., and Harper, J. W. (1997) *Cell* **91,** 209–219